Available online at www.sciencedirect.com
SCIENCE DIRECT®
ELSEVIER
Nuclear Instruments and Methods in Physics Research A 525 (2004) 458–464
NUCLEAR INSTRUMENTS & METHODS IN PHYSICS RESEARCH Section A
www.elsevier.com/locate/nima

Novel thin window design for a large-area silicon strip detector

O. Tengblad[a,*], U.C. Bergmann[b], L.M. Fraile[a,c], H.O.U. Fynbo[d], S. Walsh[e]

[a] *Instituto de Estructura de la Materia, CSIC, Serrano 113 bis, Madrid E-28006, Spain*
[b] *ISOLDE, CERN, CH-1211 Genève 23, Switzerland*
[c] *Deipartmento de Física Atómica, Molecular y Nuclear, Universidad Complutense, Madrid E-28040, Spain*
[d] *Institut for Fysik og Astronomi, Aarhus Univ., DK-8000 Aarhus C, Denmark*
[e] *Micron Semiconductor Ltd., Sussex BN15 8UN, England, UK*

Received 15 January 2004; accepted 15 January 2004

Abstract

A novel design to achieve a ultra-thin dead layer for large-area Si strip detectors is presented. The traditional contact layer making up the strip is here replaced by a grid covering only 2% of the strip area. The dead layer is thus (over 98% of the active surface) reduced to become the implantation depth only. Furthermore, the implantation depth has been reduced from 400 to 100 nm.

PACS: 29.40.Wk; 29.40 Gx; 29.30.Ep

Keywords: Large-area segmented detectors; Charged-particle spectroscopy; Dead layer effects; Thin window; Double-sided silicon strip detectors

1. Introduction

Large-area segmented Si-detectors for charged-particle spectroscopic applications have become available and are being increasingly used in the course of the last 10 years. Apart from very significant improvements, this development has also brought new challenges, e.g. a much increased number of electronics channels to be handled by the data acquisition system [1]. Typical examples of applications are studies of β-delayed particle emission, in particular when multi-particle final states have to be detected [2–8]. In a recent paper, we have discussed another problem with an often used Double-Sided Si Strip Detector (DSSSD) design when this is used in compact geometry to detect low-energy particles [9]. The dead layer from the contact and implantation layers of the DSSSD induces a non-linear energy loss of charged particles impinging on the detector, and results in effective trigger thresholds that depend on the incident particle type, energy and angle. A method of how to compensate for the energy loss of particles traversing the dead layer, based on a modified energy calibration procedure, is presented in Ref. [9].

In the present paper, we wish to address the problem of increased thresholds induced by the thickness of the entrance window by presenting a novel design of a DSSSD with a much reduced

*Corresponding author. Tel.: +34-915616800/3002; fax: +34-915855413.
E-mail address: imtot4a@iem.cfmac.csic.es (O. Tengblad).

0168-9002/$ - see front matter © 2004 Elsevier B.V. All rights reserved.
doi:10.1016/j.nima.2004.01.082

dead layer. In Section 2.1 the new design is introduced, in Section 2.2 its performance is discussed and compared to the old design, and in Section 2.3 the improvements brought through by the new detector design are illustrated in a realistic application in an on-line experiment.

2. The detector

As a starting point for this development we have used the DSSSD of Design W from Micron Semiconductor Ltd. [10]. This detector has $50 \times 50\,\mathrm{mm}^2$ total active area, divided into 16 strips of $3 \times 50\,\mathrm{mm}^2$ on the front face and 16 similar orthogonal strips on the back, making up 256 pixels of $3 \times 3\,\mathrm{mm}^2$ each. The strips are made up by hard B implantation to a depth of 400 nm, followed by a 200 nm Al conducting layer, resulting in a total detector dead layer of some 630 nm Si equivalent as tested with alpha standard sources. However, as discussed in detail in Ref. [9], the actual effect of this dead layer depends upon the particle impact angle on the detector. Using a point-like source at 25 mm distance the average dead layer becomes 770 nm Si equivalent layer. With a typical electronic trigger threshold of the order of 200 keV this results in an alpha energy cut-off in the range of 400–600 keV, depending upon which strip has been hit, and hence preventing the detection of low-energy particles (see Fig. 2 in Ref. [9]).

2.1. New design

Since the time when the Design W was created the implantation technique has improved, and MICRON Semiconductor can nowadays produce performing strip detectors by using an implantation depth of only 100 nm (type Y process). This in combination with a standard contact layer would already reduce the dead layer by a factor of 2. However, the question was whether the thickness of the conducting layer could be reduced as well. The challenge was to achieve a sufficiently effective charge collection by just applying a grid contact covering a certain percentage of the strip area, instead of covering the full strip with a 200 nm thick Al contact. Particles hitting exactly on the grid will suffer a different dead layer than the rest, and thus will have slightly different energy deposition in the detector active layer. Therefore, an optimum between an even charge collection over the surface and a minimum grid occupation had to be found.[1]

Different prototype designs were made. The final choice is illustrated in Fig. 1. The contact is obtained by a metal grid of 1500 μm pitch and 30 μm width over an element pitch of 3120 μm. In this way, the metal grid covers only 2% of the active surface. This reduces the series resistance to about $100\,\Omega/\square$, while retaining almost the full thin window. Moreover, the effect of the additional dead layer thickness due to the grid is negligible for high-energy particles and gives an acceptable distortion of only 2% in the case of low-energy particles.

The new design, as shown in Fig. 1, has been implemented in two new DSSSDs. The detectors have a $50 \times 50\,\mathrm{mm}^2$ active area with 16 strips of $3 \times 50\,\mathrm{mm}^2$ implanted on the front face, with a 100 nm p^+-doping depth on the n-type Si bulk and the contact grid described above. The back side of the detectors consists of 16 orthogonal n^+-strips implanted using the previous design, with 400 nm doping depth and a 200 nm Al contact. The thickness chosen for both detectors was 60 μm as they are found to be very stable, with low noise in spite of their higher capacitance and have minimum response to β-particles, which would otherwise disturb the low energy detection capability in β-decay applications that are of our main interest.

2.2. Detector performance

The performances of the two detectors produced with the new design are similar. In Fig. 2 the response of one of them to a commercial triple alpha source (^{239}Pu, ^{241}Am, and ^{244}Cm; 1 kBq/isotope) is shown. The detectors were

[1] As the main aim of our experiments is the detection and energy determination of low-energy particles, we have not considered an eventual degradation of the timing response of the detector.

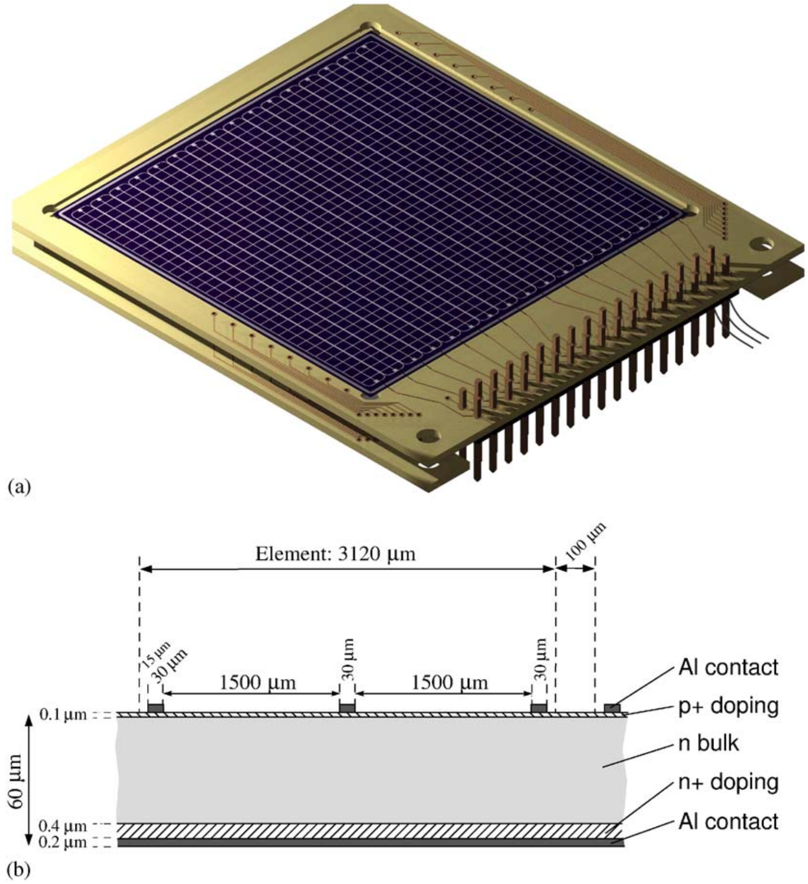

Fig. 1. The new thin-window design of DSSSD (Micron Semiconductor Ltd). (a) An illustration of the detector mounted as a $\Delta E - E$ telescope is shown. (b) Display of a sketch of the ΔE-detector profile is shown. The design is of 50×50 mm^2 active area with 16 3×50 mm^2 strips implanted on the front face, using the new design i.e. 100 nm p^+-doping depth, and an Al contact grid covering 2% of the active surface and, orthogonally on the back face, n^+-strips implanted using the previous design, i.e. 400 nm n^+-doping depth + 200 nm Al-contact.

mounted with the p^+-side, negatively biased, facing the source. Typical bias for total depletion of a 60 μm thick detector is 15 V, the detectors were overbiased to 25 V to match the leakage current of 48 nA at full depletion measured by the producer. The leakage current was stable at this value over the 8 days of experiment. These spectra were recorded as part of the calibration procedure of the experiment discussed in Section 2.3. The non-collimated source was placed in the centre of the cubic detector mount shown in Fig. 4b, at the position of the collection foil used to collect the low-energy radioactive beam during the experiment. The source was tilted 45° with respect to the plane of the detector. The distance between the source and the detector was 56 mm. Fig. 2a illustrates the response in an individual strip (i.e. one readout channel of the detector). The full detector response, i.e. the combined spectrum obtained by computer adding of the 16 front readout channels, is shown in Fig. 2b, which explains the factor of 16 difference in statistics. The resolution expressed as the full-width at half-maximum (FWHM) obtained in this particular environment is 35 keV.

A comparison of the corrections needed to account for the dead layer in the previous design W and the newly built detectors is displayed in

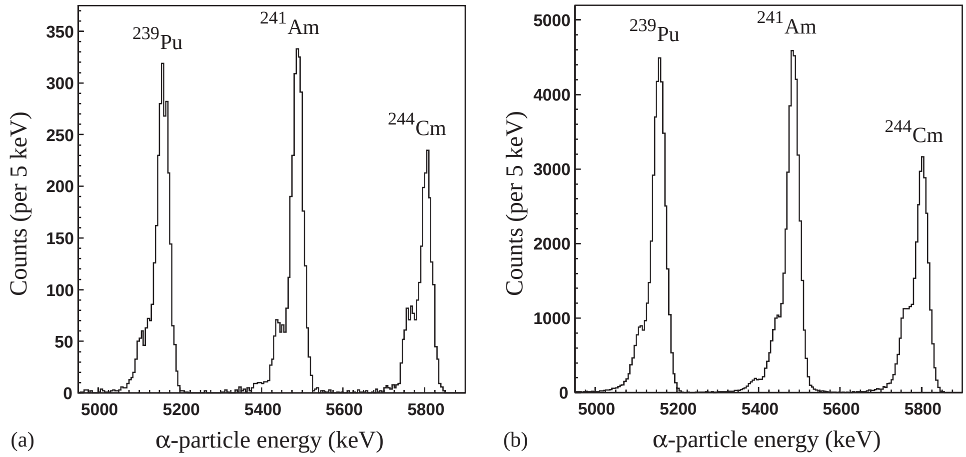

Fig. 2. Response of the new detector design to a triple alpha source (^{239}Pu $E_\alpha = 5.155(73\%)$, $5.143(15\%)$, $5.105(12\%)$, ^{241}Am $E_\alpha = 5.486(85\%)$, $5.443(13\%)$, and ^{244}Cm $E_\alpha = 5.805(77\%)$, $5.763(23\%)$ MeV). (a) The response in a single strip is shown, while in (b) the full detector response is displayed. The average resolution expressed as the FWHM obtained under experimental conditions and dead layer correction is 35 keV (see Fig. 3b for details).

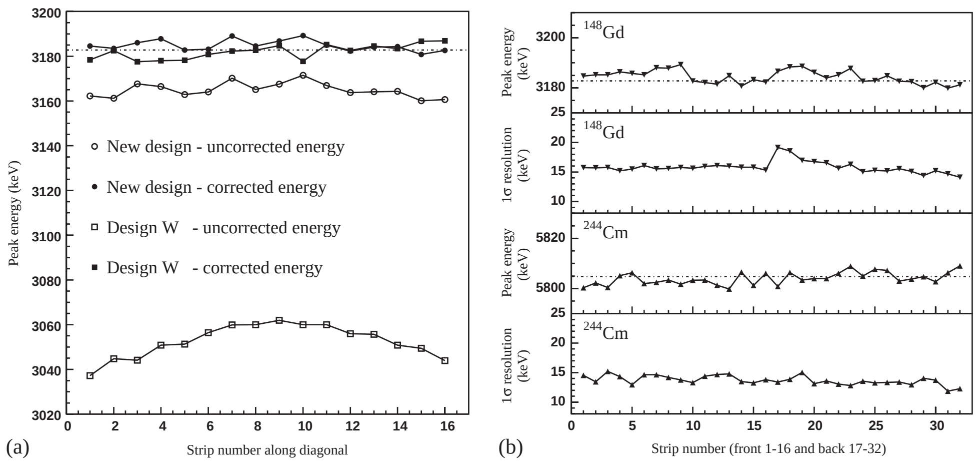

Fig. 3. Detector performances. In (a) is compared the needed dead-layer correction for the two detector designs, to obtain the right peak position at 3180 keV alpha energy. (b) The peak position (after dead layer correction) and 1σ resolution fitted for each individual strip of the new design at two different energies, ^{148}Gd(3.183 MeV) and ^{244}Cm(5.805 MeV) is shown.

Fig. 3a. The effects of the different dead layer become apparent by observing, on the one hand, the distribution of the energy loss as a function of the impact angle and, on the other hand, the overall size of the correction needed. In the present geometry the correction required (at $E_\alpha = 3180$ keV) for the Design W detectors is dependent upon the strip number and varies in the range 120–145 keV. On the contrary, with the new design we obtain a flat distribution over the detector surface and only a minor correction of ~ 20 keV is needed. In Fig. 3b the peak position and 1 σ-resolution for each strip of the new design is presented at two different energies (^{148}Gd(3.183 MeV) and ^{244}Cm(5.805 MeV)). The deviations between strips are small, which allows us to combine the data from all strips without losing accuracy.

It should be underlined that the data presented above were obtained under fully realistic conditions during setting up and calibration of an on-line experiment. Also, it should be stressed that the differences in performance of the two DSSSD designs become even more important for particles of lower energy. To illustrate this, we present in the next subsection some data obtained during the on-line experiment.

2.3. On-line experiment

To demonstrate the remarkable improvement in low energy particle detection obtained with the new detectors, we will use data from recent experiments studying the β-decay of ^{9}Li [5,11] performed at the ISOLDE facility of CERN. Data were taken at two separate occasions a year apart using two slightly different set-ups. At the first occasion standard DSSSDs of Design W from Micron Semiconductor Ltd. were used. Fig. 4a shows a photograph over the LA1 beamline in the ISOLDE (CERN) experimental hall during the second experiment. The set-up intended for charged particle detection (Fig. 4b) was built up of five Si detector telescopes occupying five of the faces of a cube of $10 \times 10 \times 10$ cm^3. Each of the telescopes consisted of a ΔE DSSSD detector backed up by a thick single area Si detector. Two of the ΔE DSSSD detectors were of the new thin-window design discussed in this paper, whereas the other three were of standard Design W. The black paddles in the frame surrounding the vacuum chamber, are parts of the TONNERRE [12] scintillator detector used here for detecting delayed neutrons in coincidence with charged particles by Time-of-Flight (ToF) technique. For all DSSSD detectors the same kind of 16 channel integrated electronics, $2 \times$ MPR-16 preamplifier connected via 2 m long non-shielded twisted pair cables to the $2 \times$ STM-16 shaper and timing filter amplifier, from the company MESYTEC [13] were used.

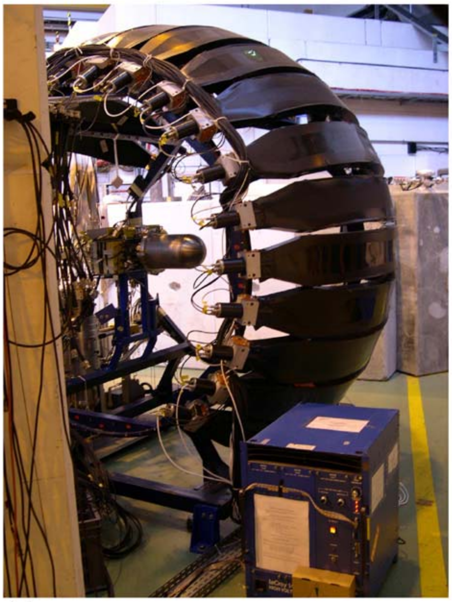
(a)

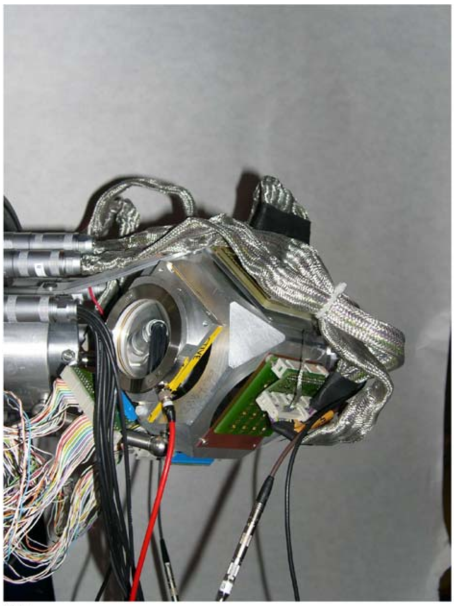
(b)

Fig. 4. The experimental situation under which parts of the data presented here were recorded. (a) Shows a photograph of the ISOLDE experimental hall, beamline LA1, ending with a bell-shaped vacuum chamber, where the charged particle set-up shown in (b) was situated. The charged-particle set-up included five telescopes building up a cube of $10 \times 10 \times 10$ cm^3. Two of the telescopes used (as ΔE DSSSD-detector) the new thin window design discussed in this paper, the other three used standard Design W DSSSDs. The black paddles in the frame surrounding the vacuum chamber are parts of the TONNERRE n-ToF detector applied here to detect delayed neutrons in coincidence with charged particles.

The impressive improvement of the cut-off at low energies and its impact on physics experiments are illustrated in Figs. 5 and 6. The experimental results are fully discussed in reference [5]. Fig. 5 shows the ^{9}Li beta-delayed alpha spectrum obtained using a detector of the new thin-window design, overlaid by the spectrum obtained using a standard detector (dashed line). As can be seen, the improved low-energy cut-off for alpha particles is 200–250 keV, i.e. the low-energy threshold is presently determined by our electronic trigger threshold only.

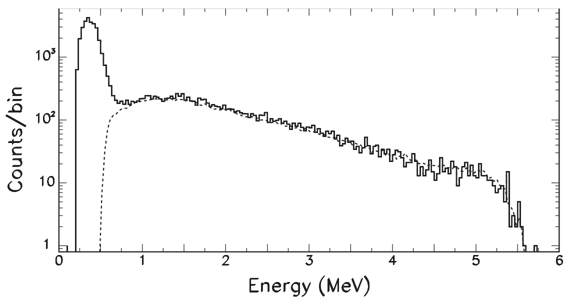

Fig. 5. Energy spectra for alpha particles from the decay of ^{9}Li. The spectrum displayed with a solid-line style was obtained using a detector of the new thin-window design, overlaid (dashed line) is the spectrum obtained using a standard detector. One should note the difference in cut-off at low energy, where only with the new design one detects the decay via the ^{8}Be(gs) + n intermediate state at 1.67 MeV excitation energy in ^{9}Be. (The two spectra are normalised to equal intensity in the region of 2–5 MeV.) For a complete discussion of the data, see Ref. [5].

The same effect is emphasized in Fig. 6. In this case, the α-particle coincidences from the breakup of the 11.81 MeV state in ^{9}Be fed in the β-decay of ^{9}Li are shown. The energy of one of the α particles is plotted versus the energy of the other one. The contribution of the ^{8}Be(gs) channel can only be seen in the data obtained using the detector of the new design (encircled area on the plot on the right-hand side), whereas this channel is not observed in data taken with the standard Design W detector (plot on the left-hand side) due to the higher threshold imposed by the 600 nm dead layer in this older detector.

3. Conclusions

The use of highly segmented detectors and detector set-ups [1] has shown to significantly improve the detection possibilities of low energy particles. The first generation of strip detectors has in comparison to standard Si-detectors the disadvantage of having a significantly thicker entrance window, in the order of 600 nm. We have discussed the influence of the thickness of the detector entrance window on the obtained experimental

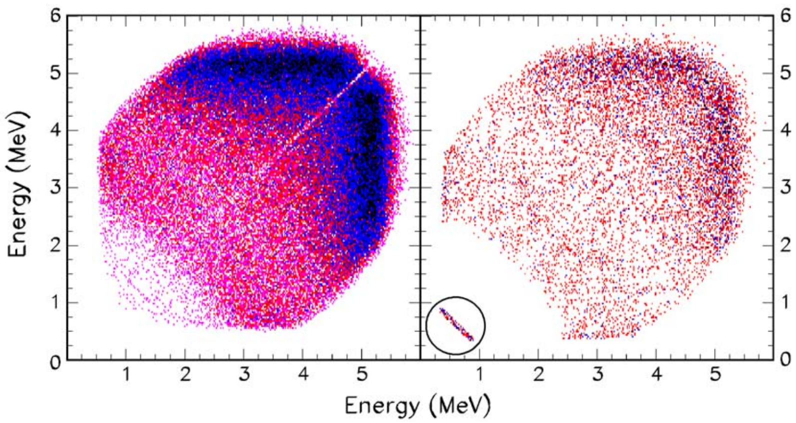

Fig. 6. Alpha particle coincidences from the breakup of the 11.81 MeV state in ^{9}Be fed in beta-decay of ^{9}Li. The energy of one of the alpha particles is plotted vs the energy of the other one. On the left side: data obtained using a standard Design W detector. On the right side: data taken with detectors of the new design. The contribution to the ^{8}Be(gs) channel (with sum of α-particle energy of about 1200 keV) can only be seen in the encircled area of the latter data. The latter data have less statistics due to shorter measuring time). For a complete discussion, see Ref. [5].

data when studying low-energy charged particles. A new novel mask design for making DSSSD detectors with ultra-thin entrance window, 100 nm only, is presented and the performance of these new detectors is demonstrated. The stability of the detectors over the full detector surface as well as an excellent energy resolution is shown. Finally, we illustrate, using data from an on-line experiment, the remarkable improvements of the experimental results obtained with the new detector.

Acknowledgements

This work was partly financed by the Spanish Ministry of Science and Technology under Project AEN1999-1046-C02-01.

References

[1] O. Tengblad, et al., Nucl. Phys. A 701 (2002) 222c.
[2] H.O.U. Fynbo, et al., Nucl. Phys. A 677 (2000) 38.
[3] U.C. Bergmann, et al., Nucl. Phys. A 692 (2001) 427.
[4] E. Gete, et al., Phys. Rev. C 61 (2000) 064310.
[5] Y. Prezado, et al., Phys. Lett. B 576 (2003) 55.
[6] H.O.U. Fynbo, et al., Phys. Rev. Lett. 91 (2003) 82502.
[7] H.O.U. Fynbo, et al., Eur. Phys. J. A 15 (2002) 135.
[8] H.O.U. Fynbo, et al., Nucl. Phys. A 718 (2003) 541.
[9] U.C. Bergmann, H.O.U. Fynbo, O. Tengblad, Nucl. Instr. and Meth. A 515 (2003) 657.
[10] MICRON Semiconductor, Lancing, Sussex, UK, http://www.micronsemiconductor.co.uk/.
[11] CERN-INTC-2003-009, http://doc.cern.ch//archive/electronic/cern/preprints/intc/public/intc-2003-009.pdf.
[12] A. Buta, et al., Nucl. Instr. and Meth. A 455 (2000) 412.
[13] Mesytec gbr, Wernher-von-Braun-str. 1, 85640 Putzbrunn, Germany, http://www.mesytec.com/.